Amphiphiles formed from synthetic DNA-nanomotifs mimic the step-wise dispersal of transcriptional clusters in the cell nucleus

Xenia Tschurikow,[†,‡,#] Aaron Gadzekpo,[†,‡,#] Mai P. Tran,[¶,§] Rakesh Chatterjee,[‖,⊥] Marcel Sobucki,[†] Vasily Zaburdaev,[‖,⊥] Kerstin Göpfrich,[¶,§] and Lennart Hilbert[*,†,‡]

†*Institute of Biological and Chemical Systems, Karlsruhe Institute of Technology, Eggenstein-Leopoldshafen 76344, Germany*

‡*Zoological Institute, Karlsruhe Institute of Technology, Karlsruhe 76131, Germany*

¶*Center for Molecular Biology of Heidelberg University (ZMBH), Heidelberg 69120, Germany*

§*Max Planck Institute for Medical Research, Heidelberg 69120, Germany*

‖*Max Planck Zentrum für Physik und Medizin, Erlangen 91058, Germany*

⊥*Chair of Mathematics in Life Sciences, Friedrich-Alexander Universität Erlangen-Nürnberg, Erlangen 91058, Germany*

#*These authors contributed equally*

E-mail: lennart.hilbert@kit.edu

Supporting Information Available

Methods and Materials

Zebrafish husbandry and collection of embryos

All zebrafish husbandry was performed in accordance with the EU directive 2010/63/EU and German animal protection standards (Tierschutzgesetz §11, Abs. 1, No. 1) and is under supervision of the government of Baden-Württemberg, Regierungspräsidium Karlsruhe, Germany (Aktenzeichen35-9185.64/BH KIT).

Immunofluorescence staining of zebrafish embryo animal caps

Zebrafish embryos in the sphere stage were collected as previously explained.[27] In particular, wild-type adult fish (AB strain from the Zebrafish International Resource Center, maintained at the European Zebrafish Resource Center) were set up for spontaneous mating, eggs were collected and chorions removed by treatment with pronase. Embryos were maintained in 0.3X Danieau's solution, and transferred into 0.3X Danieau's supplemented with 2% formaldehyde and 0.2% Tween-20 for fixation. Permeabilization was carried out by 15 min exposure to 0.5% Triton X-100 in phosphate-buffered saline (PBS, Dulbeccos's formulation) at room temperature. After two washes in PBS with 0.1% Tween-20 (PBST), 30 min of blocking with 4% Bovine Serume Albumin (BSA) in PBST followed. Samples were then incubated at 4°C overnight with primary antibodies against Pol II S2P (Abcam ab193468, rabbit IgG monoclonal, clone EPR18855, dilution 1:300) and Pol II S5P (Active Motif, rat IgG monoclonal, clone 3E8, dilution 1:300) in 4% BSA-PBST. After 3 washes in PBST, the samples were again incubated overnight with secondary antibodies (ThermoFisher, anti-rat polyclonal conjugated with Alexa 594, dilution 1:300; ThermoFisher anti-rabbit polyclonal conjugated with STAR RED, dilution 1:300) in 4% BSA-PBST. Samples were washed 3 times in PBST, post-fixed in 2% formaldehyde in PBS for 15 min at room temperature,

again washed 3 times in PBST. Mounting was carried out by placing animal caps immersed in non-setting mounting media (VectaShield H-1000) supplemented with 1.6 μM Hoechst 33342 between adhesive strips spaced 2-4 mm apart, which were covered with thickness-selected #1.5 glass cover-slips. The assembled sample was then sealed with nail polish.

Preparation of flow cells on microscope slides

Flow cells were prepared by placing strips of double-sided tape on glass microscope slides to form several channels. To block surfaces for binding, the flow cells were incubated with 2% bovine serum albumin (BSA) for 5 min. After removing the remaining solution with a chemical wipe, the microscope slides were air-dried. Then cover slips were placed on the microscope slides. For imaging, the flow cell channels were filled with sample solution and sealed with silicone grease.

Preparation of DNA-nanomotif suspensions

Oligonucleotide preparation.

Oligonucleotides were purchased from biomers.net and Integrated DNA Technologies (IDT) with purification by standard desalting (unmodified strands) or HPLC (fluorophore-tagged strands). The individual strand sequences were taken from previous work[5] and adapted as detailed in Supplementary Table S1. Individual oligonucleotide preparations were dissolved in 1X TE at 200 μM and stored at -20°C up until preparation of mixtures needed for a given experiment.

Nanomotif formation.

To produce the different nanomotifs (Figure 2A, B), the corresponding DNA-oligomers were separately mixed together in 25 μl of 2X TE with 700 mM NaCl. The solutions were then heated up with a thermocycler (Eppendorf Mastercycler X50) to 85°C for 3 min, before decreasing the temperature at a rate of -1°C/min to 40°C. How the different star-motifs affect the Y-motif droplets was investigated by first preparing all components separately (5.0 μM

Y-motif and 1.65 μM star-motif), then mixing both parts in equal proportions and heating up to 60°C before decreasing the temperature at a rate of -1°C/min. Annealed nanomotifs were used immediately.

Inhibition of amphiphile with poly-A blocker elements.

Nanomotifs were prepared separately, (10.0 μM Y-motif and 5.0 μM amphiphile-motif). Then, 4.44 μM Y-motif and 2.22 μM amphiphile-motif were mixed together with 22.2 μM of a 10-nt poly-A blocker (for sequences see Supplementary Table S1). Control solutions were prepared by the substitution of the poly-A blocker solution with an equivalent amount of water. The samples were heated up to 60°C, then the temperature was decreased at a rate of -1°C/min to 40°C before imaging the samples.

Time-lapse of amphiphile-droplet interaction.

Time-lapse experiments were performed by first preparing 20.0 μM Y-motif and 15.0 μM of amphiphile-motif in separate tubes, then mixing 10.0 μM of the Y-motif solution with 7.5 μM of the amphiphile-motif solution (concentrations in final mixture). The mixture was then added to preheated (40°C) flow cells and imaged at 40°C for up to 4 h.

Time-course of amphiphile-droplet interaction with incubation in a thermocycler.

The time-lapse experiments were repeated at 50°C, assuming that the nanomotifs reorganize faster at elevated temperature. Here, 10.0 μM of Y-motif and 15.0 μM of amphiphile-motif and control-motif were prepared separately, before mixing 5.0 μM Y-motif and 7.5 μM amphiphile-motif or control-motif together (concentrations in final mixture). Several tubes were prepared and incubated at 50°C in a thermocycler. Every 10 min, an amphiphile-motif and a control-motif sample were retrieved from the thermocycler and injected into preheated flow cells (40°C) for imaging (ambient temperature 40°C).

Titration of amphiphile-motifs.

Titration experiments were conducted by preparing 30.0 μM of Y-motifs and 22.5 μM of amphiphile-motifs and control-motifs in 3 separate tubes. Then, 6 tubes of 15 μM Y-motif

and 11.25 μM amphiphile and control-motif were mixed together. In the first tube, only 11.25 μM of control-motif were added. In the following tubes, the control-motif was replaced with amphiphile-motifs in 20%-steps, so that the last tube only contained amphiphile-motifs and Y-motifs. These tubes were then heated up to 60°C and cooled down at a rate of -1°C/min to 40°C. For imaging, the different samples were injected in prewarmed flow cells (40°C) and imaged at 40°C.

Imaging procedure.

Samples were visualized using an instant structured illumination microscope (iSIM) from VisiTech. Before injection, flow cells were heated up to 40°C. Microscopy of the samples was carried out in a heated microscope stage enclosure at a temperature of 40°C.

Microscopy and image analysis

Zebrafish embryos

Confocal microscopy images were obtained using a VisiTech iSIM microscope, which is a commercial implementation of a microscope based on the the instant-SIM principle.[37] The microscope is based on a Nikon Eclipse Ti2 microsope body. A motorized correction collar oil immersion objective (CFI SR HP Apo TIRF 100XAC Oil, NA 1.49) was used. Images were acquired with a single ORCA-Flash4.0 V3 camera with sequential acquisition of color channels for maximal positional accuracy and minimal cross-talk. To limit the analysis to conventional gene and enhancer loci, nuclei with visible miR-430-associated foci were excluded from the data set.[57,58,67]

The analysis of fluorescence intensities and shapes of Pol II clusters was carried out following our previous work,[27] using MatLab for analysis and the Open Microscopy Environment bioformats plugin for data import.[59] In brief, a two-step segmentation pipeline was applied, first segmenting cell nuclei by Otsu-thresholding of the DNA-channel, followed by robust background threshold segmentation of Pol II clusters from the Pol II Figure channel in each detected nucleus. For each detected cluster, the geometric characteristics volume

and sphericity and the mean intensities in the Pol II S5P and the Pol II S2P channel were calculated under consideration of the 3D-shape segmentation mask. Mean intensities were normalized against the median intensity of the containing nucleus to compensate for variability in sample staining and image acquisition between different nuclei and samples. Sphericity was calculated as

$$36\pi V^2/S^3,$$

where V is the volume and S the surface area of a given 3D object

The raw data and the image analysis code for Figure 1 is deposited on Zenodo: `https://doi.org/10.5281/zenodo.5242771`

Nanomotif suspensions

Nanomotifs were imaged using a water immersion objective (Apo LWD 40x WI λS DIC N2, NA 1.15). Images were recorded using dual ORCA-Flash4.0 V3 cameras with simultaneous two-channel acquisition to avoid displacement of objects due to consecutive acquisition of color channels. Time-lapse microscopy images in Figure 2G were acquired using a silicone oil immersion objective (CFI SR HP Plan Apo Lambda S 100XC Sil, NA 1.35) with simultaneous acquisition using dual ORCA-Quest cameras, which were purchased as a microscope upgrade while this study was under review.

The images were further processed with the software Fiji.[60] Raw images containing the droplets formed by Y-motifs were resliced in the z-axis to generate cubic voxels and then filtered using Gaussian Blur 3D with the parameters σ = 2,2,2 pixels for x, y, and z, respectively. To obtain image data for the volume, sphericity, and elongation of the detected droplets, the plugin MorphoLibJ was used.[61] Images were processed with the "Morphological Segmentation" tool as object images with the gradient type "Morphological", gradient radius = 2 and a tolerance = 100. Images were displayed in the "Catchment basins" format.

The background was removed by using the command "Remove Largest Object". Images were further analyzed using the tools "Analyse Regions 3D" for the volume and sphericity (surface area method = Crofton (13 dirs.), Euler connectivity = 6).

The raw data and the image analysis code is deposited on Zenodo.

Comparison of different amphiphiles (Figure 2B): `https://doi.org/10.5281/zenodo.7572656`

Blocking of poly-T amphiphiles (Figure 2C): `https://doi.org/10.5281/zenodo.7572624`

Continuous time-lapse on the microscope, 40° (Figure 2E): `\textcolor{\diffcolor}{https://doi.org/10.5281/zenodo.8088893}`

Manual time-lapse, 50° (Figure 3A and Figure S4A-C): `https://doi.org/10.5281/zenodo.7572230`

Titration poly-T amphiphile (Figure 4B-D and Figure S6A, B) `https://doi.org/10.5281/zenodo.7573452`

Surface tension measurement by the sessile droplet method (`https://doi.org/10.5281/zenodo.8089869`,`https://doi.org/10.5281/zenodo.8090349`)

Surface tension measurement by the sessile droplet method

The method used in the following to determine the surface tension of droplets from sedimentation speeds and the shape of sessile droplets is described in detail in.[38]
The sedimentation speed of a droplet is determined by a balance between viscous drag and buoyancy experienced by the droplet. In a regime of low Reynolds numbers, Stoke's law describes the drag force which allows to derive an expression for the density difference between droplet and surrounding medium:

$$\Delta\rho = \frac{9v\eta}{2R^2 g} \ . \tag{1}$$

The sedimentation speed v and radius R can be determined from microscopy images of droplets sedimenting in a flow cell. We measured the droplet radius R and the time it took the intensity maximum to pass two z-planes separated by 1.15 or 2.29 μm and calculated the sedimentation speed. For the viscosity η, we used the value for water at 43°C,[62] g is the gravitational acceleration. The density difference is linked to surface tension by the capillary length

$$L_c = \sqrt{\frac{\gamma}{\Delta\rho g}}\,, \tag{2}$$

which can be obtained by fitting the Laplace equation to the shape of sessile droplets, which balance hydrostatic pressure and surface tension. To fit this differential equation to the outline of sessile droplets, we used a MATLAB script provided with the description of the sessile droplet method.[38]

For our droplets, we obtained a sedimentation velocity of $0.189 \pm 0.017\,\mu$m/s at a radius of $1.6 \pm 0.8\,\mu$m, resulting in a density difference of $22 \pm 3\,\mathrm{kg/m^3}$ (n=7, mean±SEM). The capillary length was determined to be $155 \pm 6\,\mu$m (n=10, mean±SEM), yielding a surface tension of $5.2 \pm 0.6\,\mu$N/m (mean±SEM). Due to their small size of a few microns, our sessile droplets are not ideal for shape quantification,[63] we therefore interpret our result as a rough estimate for surface tension.

Physical properties of droplets strongly depend on temperature, salt concentration and the number and design of sticky ends. We believe that our results are broadly in line with other publications given that surface tension should increase with decreasing temperature. A recent publication[64] found, that droplets comprising the Y-motifs also used in our study have a viscosity of $\approx 0.13\,$Pas and a surface tension of $\approx 0.025\,\mu$N/m given a salt concentration of [NaCl]=350 mM at a temperature of 63.7°C. Another publication[65] assessed the influence of salt concentration (0.25-1 M NaCL) on physical properties of droplets comprising nanomotifs with 4 arms and sticky-ends with 7 base pairs at a temperature of 20°C. Here, viscosities in

the range $24 - 88$Pas and surface tensions in the range $1.23 - 3.7\mu$m/N were measured using sedimentation velocities (around 0.33 μm/s for droplets with radius 3.51 μm), micro- and bulk-rheology.

Dynamic Light Scattering measurement of droplet volume distribution

For the Dynamic Light Scattering measurement 5.0 μM Y-motif and 1.65 μM amphiphilic or control star-motif were mixed with 500 μl of 2X TE with 700 mM NaCl and filled up to 1 ml. For each condition 2 repeats were performed. The solutions were heated up to 85°C for 3 min, before decreasing the temperature at a rate of -1°C/min to 40°C. The samples cooled down to room temperature.

Further measurements were performed using a Zetasizer Nano ZS from Malvern Panalytical. The measurements were carried out at a temperature of 25°C. A value of 1.58 was selected for the refractive index of the DNA material inside the droplets. For the dispersant, a refractive index of 1.33 and viscosity of 0.8882 mPs was chosen, assuming properties close to PBS. Due to the heterogeneous droplet population and ripening during the measurements, the evaluation script struggled to produce a probability distribution for the measured size, however, the average diameter could be reproducibly obtained. For the subsequent evaluation, the average diameter was obtained from two repeats with three measurements each.

Interacting-particle model

Interacting-particle dynamics in ReaDDy

Brownian dynamics is a common approach to describe particles subject to both deterministic forces in a Newtonian sense and stochastic forces that result in Brownian motion. Particle motion is determined by an overdamped version of a stochastic differential equation called Langevin equation:

$$\begin{aligned} \frac{d\vec{x}}{dt} &= -D\frac{\nabla V\left(\vec{x}\right)}{k_B T} + \sqrt{D}\vec{\eta}\left(t\right) \ , \\ \left\langle \vec{\eta}\left(t\right)\right\rangle &= 0 \ , \\ \left\langle \vec{\eta}\left(t\right)\vec{\eta}\left(t'\right)\right\rangle &= 2\delta\left(t-t'\right) \ . \end{aligned} \tag{3}$$

The particle position is denoted by $\vec{x}$, the diffusion constant by D, the Boltzmann constant times temperature by $k_B T$ and a delta-correlated Gaussian noise term by $\vec{\eta}$. Interactions are summed up in the potential V. The fluctuation-dissipation theorem ($\sigma^2 = \xi k_B T$) and specifically the Einstein relation $\left(D = \frac{k_B T}{\xi}\right)$ were applied to relate the friction coefficient ξ, the noise amplitude σ, and the diffusion constant. The noise contribution is drawn from a Gaussian with zero mean and variance of one $\vec{\eta}_i \sim \frac{\mathcal{N}(0,1)}{2}$.

ReaDDy (short for Reaction Diffusion Dynamics) is a software package capable of numerically integrating the Langevin equation (3) for individual particles. Importantly, it also allows the user to include various potentials for interactions between the particles and chemical reactions that can convert, create, or delete particles. This kind of simulation is often referred to as interacting-particle reaction dynamics (iPRD) and has proven versatile enough to model and simulate a variety of biochemical systems. ReaDDy, in version 2.0.12, was used for all simulations based on Brownian dynamics. A more in-depth introduction to ReaDDy can be found in.[66]

The Euler-Maruyama method is used to integrate the Langevin equation. The evolution from a position $\vec{x}\left(t\right)$ to $\vec{x}\left(t+dt\right)$ can be written as:

$$\vec{x}_i\left(t+dt\right) = \vec{x}_i\left(t\right) + \frac{D}{k_B T}\vec{F}_i\left(t\right)dt + \sqrt{2Ddt}\mathcal{N}\left(0,1\right) \ , \tag{4}$$

where the effects of external forces and interaction forces with other particles are summed up in $\vec{F}$:

$$\vec{F} = -\nabla\left(\sum_{external} U_{ext} + \sum_{interactions} U_{int}\right) \ . \tag{5}$$

A variety of potentials can be used to model inclusion or exclusion effects and attraction or repulsion between particles. Examples include Lennard-Jones or harmonic pair potentials, spherical barriers or inclusion potentials. A detailed summary can be found on the website of ReaDDy (`https://readdy.github.io/system.html#potentials`).

ReaDDy is accessible via a Python interface, however, the core functionality is written in C++. This way, the user benefits from Python's accessibility without sacrificing optimisation for speed. The script used for the simulations is available on Zenodo: `https://doi.org/10.5281/zenodo.7957242`.

Parameters of simulation

The droplet simulation is a coarse-scale, effective model of the DNA-nanomotif system. Our aim was to find a parameter space for particle interaction that reproduces the experimental results. Particle concentrations and sizes are thus not directly comparable to the DNA-system.

Our model for the Y-motif is a spherical particle with diffusion constant $D_y = 0.0352\,\mathrm{nm}^2/\mathrm{ns}$ obtained from the Einstein relation. Interaction with other Y-motifs is defined by a harmonic well potential:

$$V = \begin{cases} \frac{1}{2}k_{wp}\left(d - r_0\right)^2 - e, & \text{if } d < r_0\ , \\ \frac{e}{2}\left(\frac{r_c - r_0}{2}\right)^{-2}\left(d - r_0\right)^2 - e, & \text{if } r_0 \leq d < r_0 + \frac{r_c - r_0}{2}\ , \\ -\frac{e}{2}\left(\frac{r_c - r_0}{2}\right)^{-2}\left(d - r_c\right)^2, & \text{if } r_0 + \frac{r_c - r_0}{2} \leq d < r_c\ , \\ 0, & \text{otherwise}\ , \end{cases} \tag{6}$$

$$d = \sqrt{\vec{x_1}^2 - \vec{x_2}^2}\ .$$

After testing various parameter settings, we decided to use the following for our simulations:

- spring constant of repulsive part: $k_{wp} = 10^{-20}\ \mathrm{J/nm}^2$

- depth of well: $e = 2 \cdot k_B T$
- position of minimum: $r_0 = 20$ nm
- cut-off distance: $r_c = 30$ nm

The amphiphile particle comprises of one particle identical to the Y-motif model and one "tail particle" that is repulsed by all other particles via a harmonic potential:

$$V = \begin{cases} \frac{1}{2} k_{hr} \left(d - r_c\right)^2 , & \text{if } d < r_0 \ , \\ 0, & \text{otherwise} \ , \end{cases} \qquad d = \sqrt{\vec{x_1}^{\,2} - \vec{x_2}^{\,2}} \ . \tag{7}$$

The following parameters were used:

- spring constant: $k_{hr} = 10^{-20}$ J/nm^2
- cut-off distance: $r_c = 30$ nm

The diffusion constant of the "tail particle" was set to $D_y = 0.0175$ nm^2/ns to model a larger effective volume.

A bond potential defines the interaction between the two sub-particles of our amphiphile model:

$$V = k_b \left(d - r_0\right)^2 \ , \qquad d = \sqrt{\vec{x_1}^{\,2} - \vec{x_2}^{\,2}} \ . \tag{8}$$

Here, we used the following parameters:

- spring constant: $k_{hr} = 10^{-20}$ J/nm^2
- minimum distance: $r_0 = 31$ nm

All particles are also subject to an inclusion potential defined by:

$$V = \begin{cases} \sum_{i=1}^{d} \frac{1}{2} k_{bp} d\left(\vec{x}_i, C_i\right)^2, & \text{if } \vec{x}_i \in C_i \ , \\ 0, & \text{otherwise} \ . \end{cases} \tag{9}$$

The term $d\left(\vec{x}_i, C_i\right)^2$ represents the shortest distance between the particle position $\vec{x_i}$ and the boundary of a cube $C_i = [origin_i, origin_i + extent_i]$.

We used the following parameters:

- spring constant: $k_{bp} = 10^{-20}$ J/nm^2
- extent of box = 800 nm

The box was centered in a simulation volume of extension 1x1x1 μm.

Simulation of time series

Simulations for the time series comprised of two steps: In the first step, 450 Y-motif particles were randomly placed in a spherical volume of radius 200 nm and simulated for 10^6 time steps of 0.5 ns and 60°C. The final configuration containing preformed droplets was used for the second step. Here, 450 additional Y-motifs (as control case) or amphiphile-motifs were randomly added into a volume of 0.8x0.8x0.8 μm, without creating particle overlaps. The system was then simulated for $5 \cdot 10^6$ steps of 0.5 ns and a reduced temperature of 40°C. This process was repeated for 10 independent simulations, using the standard interaction parameters defined above.

Simulation of titration

Simulations for the titration split 450 particles between the models for Y-motif and amphiphile-motif. The amphiphile percentage was increased from 0% to 100% in steps of 10%. 20 independent simulations for each case were produced containing 10^6 time steps of 0.5 ns at

a temperature of 60°C. Initially, particles were randomly distributed in a spherical volume of radius 200 nm. Interaction parameters were identical to the ones discussed earlier.

Detection and evaluation of simulated droplets

Droplets in the simulations were detected by using the DB scan algorithm as implemented in the python package scikit-learn (version 1.1.2). If not specified otherwise, a minimum sample number of 10 and a maximum distance of 40 nm between particles were used.

As a proxy for the volume of each droplet, the number of particles per droplet was calculated. Alternatively, we discretized the simulation box into cubes of 10 nm edge length and counted the number of filled boxes for each droplet. This approach introduces a limited resolution, as one voxel can contain multiple particles and structure is not resolved for scales smaller than the box length.

Sphericity was calculated by using the python package jakteristics in version 0.5.0 (see `https://github.com/jakarto3d/jakteristics`) which calculates the sphericity of a point cloud as ratio between the largest and the smallest eigenvector.

Lattice model

The dispersal of Y-motif droplets by an addition of amphiphile-motifs was also studied by numerical simulation in a square lattice system with specific particle-particle interaction and excluded volume effects. The dynamic Monte-Carlo simulation is performed on a 64×64 two-dimensional lattice with periodic boundary conditions. Y-motifs are represented by T-shaped particles which occupy four sites in the lattice while amphiphiles and controls are denoted by cross shaped particles which occupy five lattice sites. The negative arm (red) of the amphiphiles is replaced by neutral arm (arm with a white dot in Figure 5E) for controls. We start from a random initial configuration with T-shaped particle concentration of 0.020 and amphiphilic concentration of 0.030. Due to the arrest effect of the particles resulting from their shape, a higher concentration of cross shaped motifs compared to the T-shaped motifs is

needed to observe the amphiphilic effect in the system. The attractive interaction between any two arms except the negative arm is given by $3.0k_BT$ while the repulsive interaction between the negative arm and other is $6.5k_BT$, where T is the explicit system temperature and the Boltzmann constant (k_B) is taken as unity. The neutral arm is non-interacting, it only occupies a lattice site. A single Monte Carlo sweep (MCS) is defined when on average each DNA motif is attempted to move to any of its four directions with equal probability representing translational diffusion and attempted to rotate by $\pi/4$ angle in either direction with equal probability as rotational diffusion. We have simulated the system for maximum of 10^8 MCS. All the movements and rotations took place using standard Metropolis algorithm, which involved change in interaction energy ΔE and the temperature T of the system. We have kept $T = 0.45$ fixed while increasing T would more likely randomize the system by thermal moves. We have measured area and circularity of the droplets from the snapshots of the system configuration using connected components function in MATLAB. To compare the results with experiment and with the Brownian dynamics simulation, we measured circularity which is analogous to sphericity in 3-dimensional system. The number of DNA motifs present in a given droplet was directly obtained via the droplet area in the unit of pixels, with each pixel representing one lattice site.

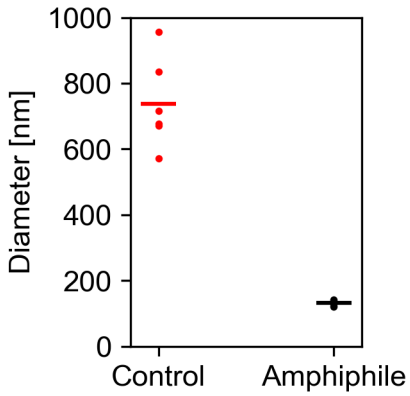

Figure S1: **Droplet diameter obtained from Dynamic Light Scattering measurement.** Using dynamic light scattering (DLS) we obtained droplet diameters of $740 \pm 50\,\mathrm{nm}$ (mean±SEM, $n = 2$ repeats with 3 measurements each) for droplets with added control motifs and $131 \pm 3\,\mathrm{nm}$ (mean±SEM, $n = 2$ repeats with 3 measurements each) with added amphiphile motifs.

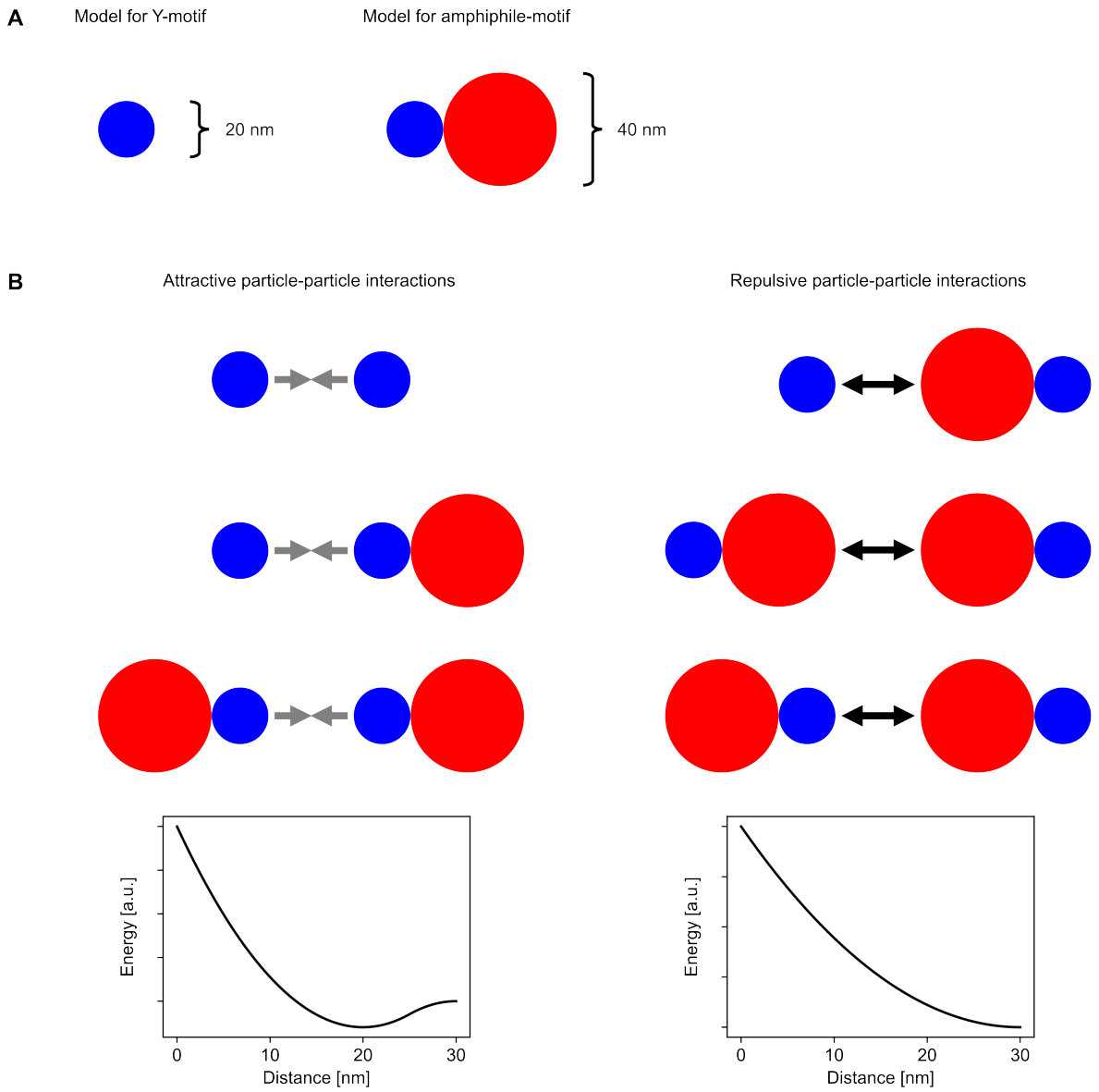

Figure S2: **Summary of sizes and interaction parameters used for interacting-particle simulations.** A) To-scale drawing of the two types of particles used in the simulation. B) Overview of attractive and repulsive particle interactions, displayed with interaction potentials that implement these interactions in the ReaDDy framework. For better visualisation, the energy axis uses arbitrary units and is not drawn to scale.

Table S1: Strand names and sequences of nanomotifs

Strand name	Sequence (5'-3')
Y-1_8	GCTCGAGCCAGTGAGGACGGAAGTTTGTCG TAGCATCGCACC
Y-2_8	GCTCGAGCCAACCACGCCTGTCCATTACTTC CGTCCTCACTG
Y-3_8	GCTCGAGCGGTGCGATGCTACGACTTTGGA CAGGCGTGGTTG
Y-2_Atto488	[Atto488]-CAACCACGCCTGTCCATTACTTCCGT CCTCACTG
S-1_0	GCTGGACTAACGGAACGGTTAGTCAGGTATG CCAGCAC
S-2_0	CTCAGAGAGGTGACAGCATTCCGTTCCGTTA GTCCAGC
S-3_0	CCATGGTCCCAAGTGATGTTTGCTGTCACCT CTCTGAG
S-4_8	GCTCGAGCCGGCGCTGTAAATTTGCGTTCAT CACTTGGGACCATGG
S-5_8	GCTCGAGCCAGACGTCACTCTCCAACTTCGC AAATTTACAGCGCCG
S-6_8	GCTCGAGCGTGCTGGCATACCTGACTTTGTT GGAGAGTGACGTCTG
S-2_Atto647N	[Atto647N]-CTCAGAGAGGTGACAGCATTCCGTT CCGTTAGTCCAGC
S-1_Phosphate	[Phosphate]-GCTGGACTAACGGAACGGTTAGTC AGGTATGCCAGCAC
S-1_Poly-T	TTTTTTTTTTTTTTTTTTTTTTTTTTTTTTTTTT TTTTTTTTTTTTTTTTTTTTTTTTTTTTTTTTTT TTTTTTTTTTTTTTTTTTTTTTTTTTTTTTGCTGG ACTAACGGAACGGTTAGTCAGGTATGCCAGC AC
Poly-A blocker	AAAAAAAAAA

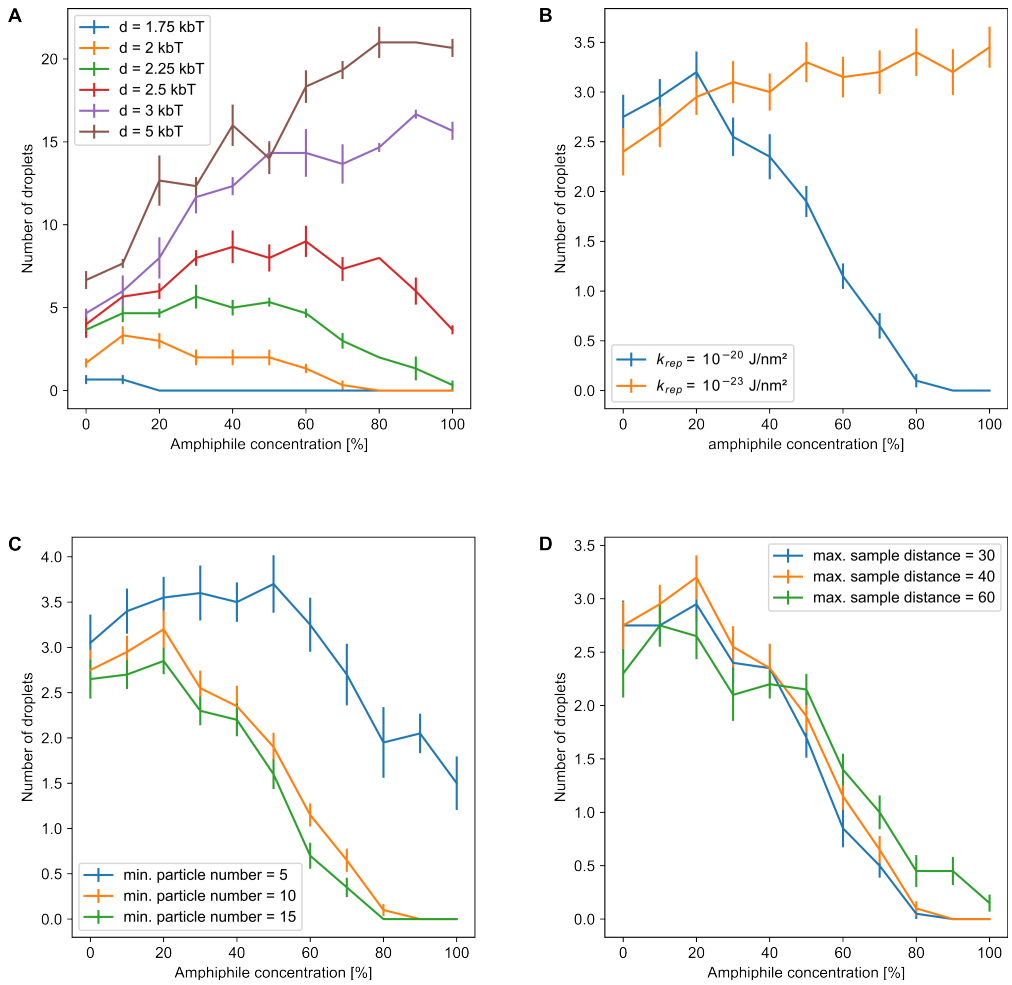

Figure S3: **The number of detected droplets in the Brownian dynamics simulation for different simulation and evaluation parameters** A) To select the parameters of the Brownian dynamics simulation, we carried out out a simulated titration experiment that places 450 particles split between Y-motif and amphiphile in a spherical volume of radius 200 nm inside a simulation box of 1 μm edge length. We then examined the final number of droplets after 10^6 time steps. As the depth of the harmonic well potential introducing attraction between simulated Y-motifs increases, the peak number of detected droplets shifts towards higher amphiphile concentrations. We selected a value of $2k_bT$ as the resulting curve resembles the experimental observation. B) Keeping the depth of the well potential fixed at $2k_bT$ and decreasing the repulsion between ampihpihle and all other particles resulted in a continuous increase of droplet number, confirming that the ration of attractive to repulsive interactions determines the shape of the curve. C) Droplets were detected with the DB-scan algorithm using a minimum number of 10 particles for classification as cluster/droplet. Changing this value by 5 particles influences the shape of the curve but not the qualitative behaviour. D) In a similar fashion, the maximum distance between particles of one cluster can be varied from the 40 nm we settled on, without changing the qualitative behaviour of the curve. Panel A averages over 3 independent simulation runs, panels B, C, and D use 20 simulation runs with well potential depth of $2k_bT$.

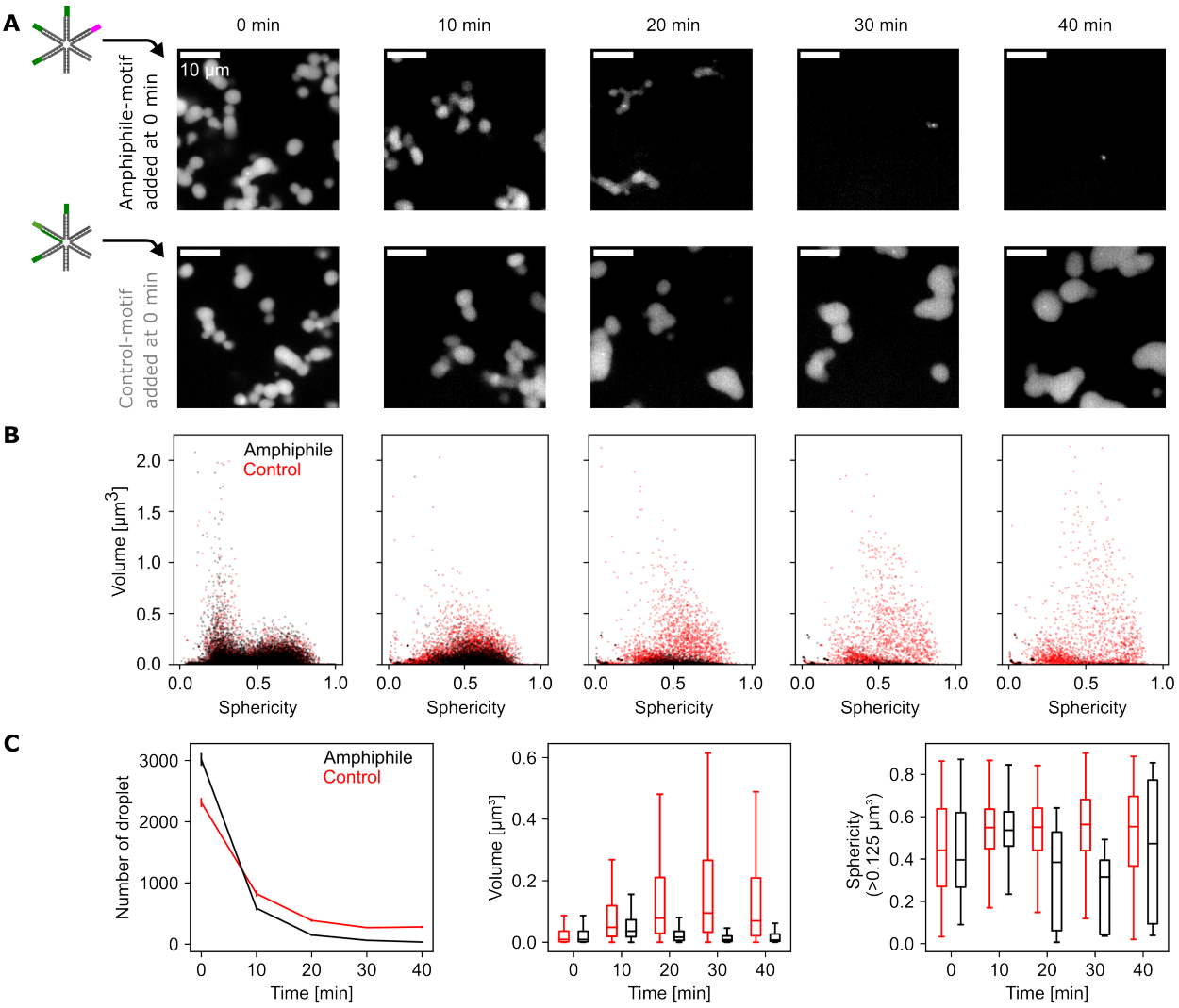

Figure S4: **Time-course of droplet dispersal upon addition of amphiphile-motifs.** A) Representative confocal microscopy sections showing the distribution of Y-motifs in flow cells prepared at 10-min time intervals after amphiphile-motifs were added to preformed Y-motif droplets (0 min). Several tubes prepared in this manner were maintained at a stable temperature of 50°C, control-motif samples were processed alongside amphiphile-motifs experiments. B) Sphericity-volume distributions obtained from the analysis of confocal images. Three-dimensional analysis was carried out in image stacks (image stacks were acquired at 7 fields of view per sample and time point, data pooled from one experiment. Number of droplets, amphiphile-motif addition: n=21123, 4110, 1044, 437, 239; control-motif addition: n=6191, 5775, 2707, 1890, 1969. C) Time courses of the number of droplets per field of view (mean±SEM, $n = 7$ fields of view per time point), volume of droplets (standard boxplots, all droplet volumes included), and the sphericity of large droplets (volumes $\geq 0.125\,\mu m^3$ included).

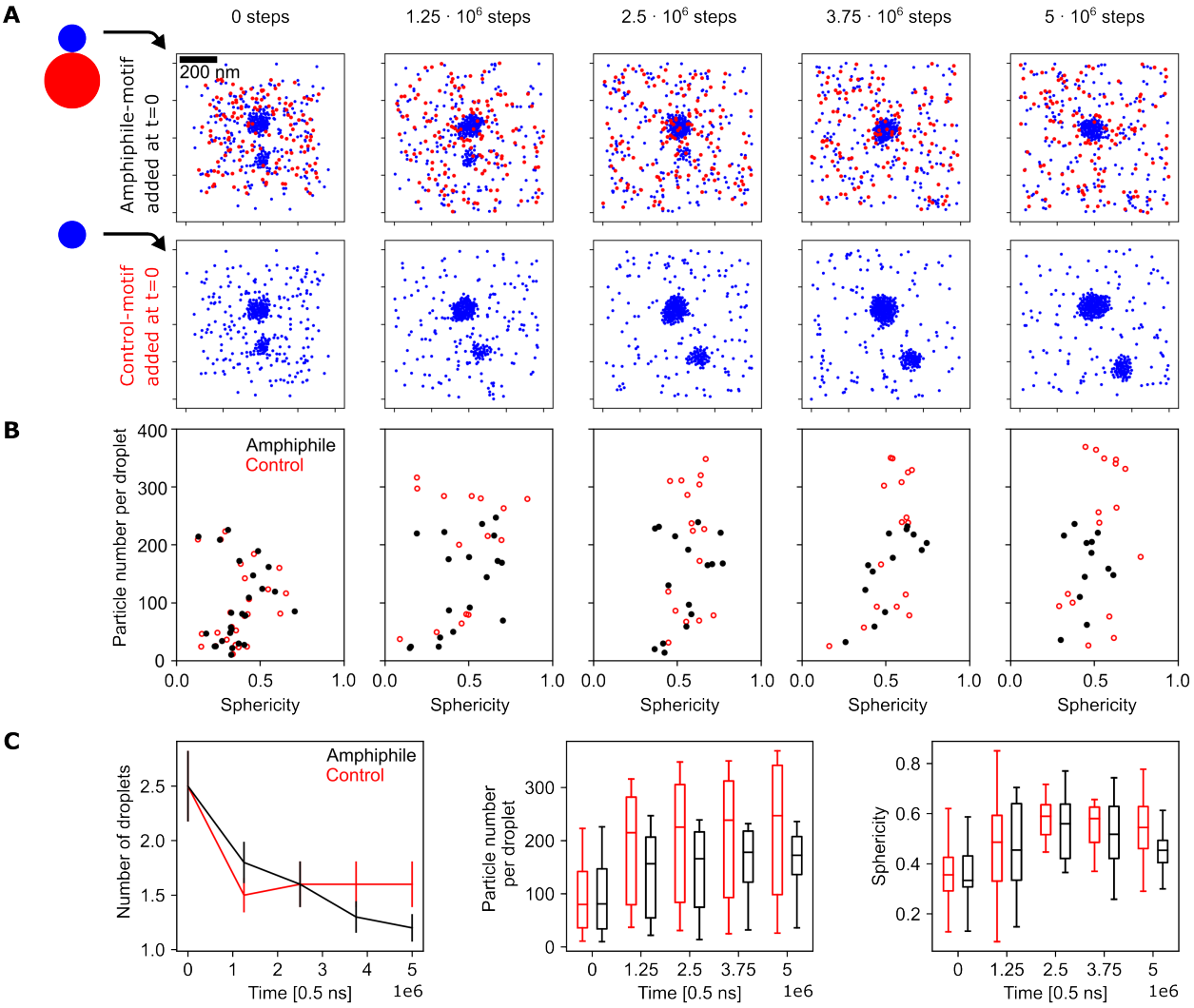

Figure S5: **Time series of amphiphile-mediated droplet dispersal obtained from interacting-particle simulations** A) To simulate the time-lapse experiment, either amphiphile-motifs or control-motifs were added to a simulation containing preformed Y-motif droplets. The preformed droplets were generated by adding 450 Y-motifs to a simulation box of 1x1x1 μm and simulating for 10^6 steps at a temperature of 60°C. Following this step, 450 additional amphiphiles or Y-motifs serving as control were added at random positions in a way that particle overlaps are prevented. $5 \cdot 10^6$ additional steps at a temperature of 40°C were then carried out. Representative z-slices of 200 nm thickness from both simulation cases are shown. Both simulations started from the same initial configuration. Control motifs were implemented identically to Y-motifs and are also displayed in blue color. B) 10 simulations for each case were used to generate distributions of sphericity versus particle number per droplet. C) The number of droplets per simulation (mean±SEM, $n = 10$ simulations) and boxplots for particle number per droplet and sphericity are shown for different time points.

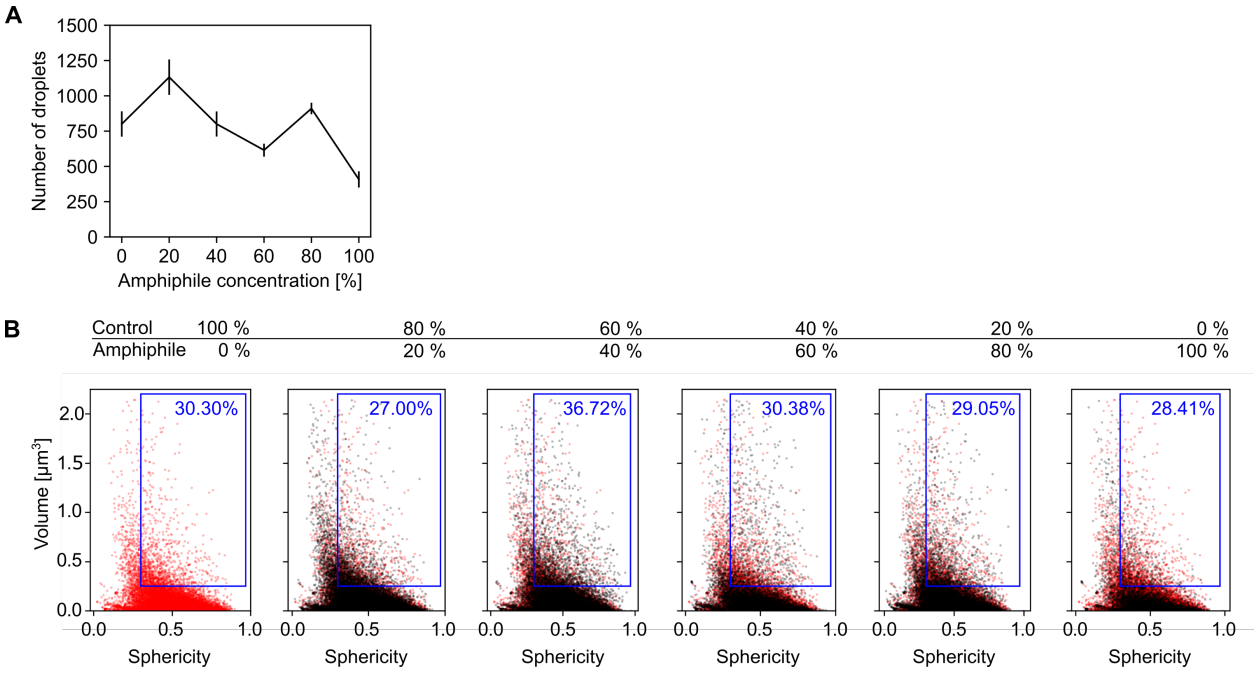

Figure S6: **Repeat of the amphiphile titration experiment.** A repeat of the titration experiment described in figure 4 resulted in similar behaviour.Y-motifs, control motifs (no poly-T extension), and amphiphile-motifs were separately prepared, mixed at different percentages of amphiphile motif, transiently heated (60°C), and injected into flow cells for microscopy (ambient temperature 40°C). As the volume fraction of amphiphile increases, the number of droplets and the percentage of larger droplets with high sphericity transiently increases. A) Changes of the number of droplets per field of view with amphiphile concentration (mean±SEM, $n = 14, 13, 14, 14, 14, 14$ fields of view). B) Sphericity-volume distributions obtained from the analysis of confocal image stacks (image stacks were acquired at up to five fields of view per sample, n=11206, 14718, 11207, 8609, 12740, 5708 droplets, data pooled from $N = 14, 14, 13, 13, 14, 14$ total fields of view pooled from three independent experimental repeats). Small droplets (volume$\leq 0.125\,\mu\text{m}^3$) were excluded in calculation of percentages.

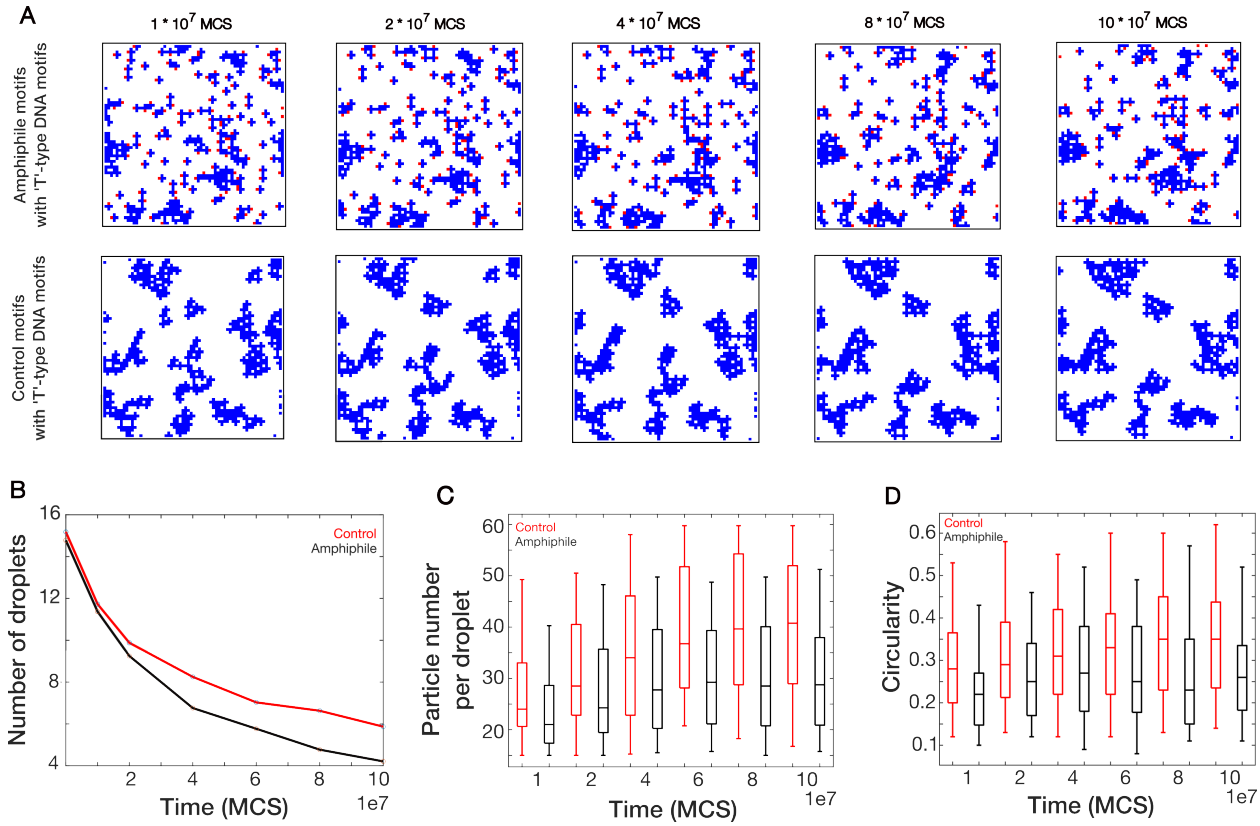

Figure S7: **Analysis of lattice simulation** A) Time-lapse snapshots for lattice simulation are illustrated when amphiphile and control motifs are introduced in the system of T-shaped DNA motifs separately. The simulations has been carried out on a 64 X 64 lattice system. B) Mean number of droplets per simulation (mean±SEM, $n = 25$ simulations) is shown as time progresses and C,D) Boxplots for time-lapse simulation are presented for particle number per droplet and circularity respectively.